

\mathcal{CP} -VIOLATING EFFECTS ON MSSM HIGGS SEARCHES*

SHRUTI PATEL^{a,b,†}, ELINA FUCHS^{c,‡}, STEFAN LIEBLER^{a,§}
GEORG WEIGLEIN^{d,¶}

^aInstitute for Theoretical Physics (ITP), Karlsruhe Institute of Technology
76131 Karlsruhe, Germany

^bInstitute for Nuclear Physics (IKP), Karlsruhe Institute of Technology
76344 Karlsruhe, Germany

^cDepartment of Particle Physics and Astrophysics
Weizmann Institute of Science, Rehovot 76100, Israel

^dDESY, Notkestraße 85, 22607 Hamburg, Germany

(Received January 22, 2018)

We study the effects of \mathcal{CP} -violating phases on the phenomenology of the Higgs sector of the MSSM. Complex parameters in the MSSM lead to \mathcal{CP} -violating mixing between the tree-level \mathcal{CP} -even and \mathcal{CP} -odd neutral Higgs states, leading to three new loop-corrected mass eigenstates h_a , $a \in \{1, 2, 3\}$. For scenarios where a light Higgs boson at about 125 GeV can be identified with the observed signal and where the other Higgs states are significantly heavier, a large admixture of the heavy neutral Higgs bosons occurs as a generic feature if \mathcal{CP} -violating effects are taken into account. Including interference contributions in the predictions for cross sections times branching ratios of the Higgs bosons is essential in this case. As a first step, we present the gluon-fusion and bottom-quark annihilation cross sections for h_a for the general case of arbitrary complex parameters, and we demonstrate that squark effects strongly depend on the phases of the complex parameters. We then study the effects of interference between h_2 and h_3 for the example of the process $b\bar{b} \rightarrow \tau^+\tau^-$. We show that large destructive interference effects modify the LHC exclusion bounds such that parts of the parameter space that would be excluded by MSSM Higgs searches under the assumption of \mathcal{CP} -conservation open up when the possibility of \mathcal{CP} -violation in the Higgs sector is accounted for.

DOI:10.5506/APhysPolBSupp.11.223

* Presented at the Final HiggsTools Meeting, Durham, UK, September 11–15, 2017.

[†] shruti.patel@kit.edu

[‡] elina.fuchs@weizmann.ac.il

[§] stefan.liebler@kit.edu

[¶] georg.weiglein@desy.de

1. Introduction

Supersymmetric (SUSY) models such as the Minimal Supersymmetric Standard Model (MSSM) or its next-to-minimal extension cannot only alleviate many shortcomings of the Standard Model (SM), but also accommodate the observed signal at 125 GeV [1, 2] as one of several Higgs bosons predicted by their extended Higgs sectors. So far, the searches for additional Higgs bosons at the LHC have been interpreted in various scenarios beyond the SM, including several supersymmetric ones. However, the most general case where \mathcal{CP} is violated and leads to mixing between \mathcal{CP} -even and -odd eigenstates has not yet been covered by those analyses. The reason for this has mainly been the lack of appropriate theoretical predictions for the Higgs production rates at the LHC for the \mathcal{CP} -violating MSSM, and of a proper prescription for taking into account relevant interference effects in Higgs production and decay. In the following, we discuss state-of-the-art cross-section predictions in the MSSM for the two main Higgs production channels at the LHC which can be used as input for future experimental analyses in \mathcal{CP} -violating Higgs scenarios [3, 4]. Additionally, an appropriate treatment of the interference effects arising in the calculation of cross section times branching ratio ($\sigma \times \text{BR}$) of a full process of production and decay of nearly mass-degenerate Higgs bosons is needed [5–8]. We review such a formalism, and subsequently study the implications of \mathcal{CP} -violating phases giving rise to Higgs mixing and interference in the process $b\bar{b} \rightarrow \tau^+\tau^-$. The resulting exclusion bounds are compared to existing experimental bounds from Run 2 of the LHC [4, 6, 7].

2. The MSSM Higgs sector with complex parameters

There are additional 105 free parameters in the MSSM, other than those from the SM. These include 12 physical, independent phases of the complex parameters of the MSSM. These phases are the ones of the soft-breaking gaugino masses M_1 and M_3 , the Higgsino mass parameter μ , and the trilinear soft-breaking couplings A_f , $f \in \{e, \mu, \tau, u, d, c, s, t, b\}$. The most restrictive constraints on the phases arise from bounds on the electric dipole moments (EDMs) of the electron and the neutron [9–11]. In the following discussion, we focus on the phases ϕ_{A_t} and ϕ_{M_3} , and their effects on the MSSM Higgs sector.

The MSSM contains two complex Higgs doublets with opposite hypercharges $Y_{\mathcal{H}_{1,2}} = \pm 1$ which induce masses for both the up- and down-type fermions. The neutral fields of the two doublets can be expressed in terms of \mathcal{CP} -even (ϕ_1^0, ϕ_2^0) and \mathcal{CP} -odd (χ_1^0, χ_2^0) components as follows:

$$\begin{aligned}\mathcal{H}_1 &= \begin{pmatrix} h_d^0 \\ h_d^- \end{pmatrix} = \begin{pmatrix} v_d + \frac{1}{\sqrt{2}} (\phi_1^0 + i\chi_1^0) \\ \phi_1^- \end{pmatrix}, \\ \mathcal{H}_2 &= \begin{pmatrix} h_u^+ \\ h_u^0 \end{pmatrix} = e^{i\xi} \begin{pmatrix} \phi_2^+ \\ v_u + \frac{1}{\sqrt{2}} (\phi_2^0 + i\chi_2^0) \end{pmatrix}.\end{aligned}\quad (1)$$

The two complex Higgs doublets possess eight degrees of freedom (d.o.f.). Three of these d.o.f. lend longitudinal components to the massive gauge bosons via the EWSB mechanism. The remaining physical d.o.f. manifest themselves as five Higgs bosons: \mathcal{CP} -even h and H , \mathcal{CP} -odd A and two charged Higgs states H^\pm . The possible \mathcal{CP} -violating phase ξ between the Higgs doublets vanishes at the minimum of the Higgs potential, and other possible phases in the tree-level Higgs potential can be rotated away. This makes the MSSM Higgs sector \mathcal{CP} -conserving at the lowest order. Besides the gauge couplings, it is fully determined by two parameters which are usually chosen as M_A or M_{H^\pm} and $\tan\beta := \frac{v_u}{v_d}$.

\mathcal{CP} -violating effects enter the MSSM Higgs sector via radiative corrections. As a result of these \mathcal{CP} -violating loop effects, the tree-level mass eigenstates $\{h, H, A\}$ mix into three \mathcal{CP} -admixed loop-corrected mass eigenstates $\{h_1, h_2, h_3\}$, with $M_{h_1} \leq M_{h_2} \leq M_{h_3}$ ¹. In evaluating processes with external Higgs bosons beyond lowest order, an appropriate prescription to account for the mixings of the tree-level states into loop-corrected mass eigenstates is required so that the outgoing particle has the correct on-shell properties, and the S-matrix is properly normalised. This is established via the introduction of finite wave function normalisation factors, denoted as the so-called \hat{Z} factors [12–14]. The non-unitary \hat{Z} matrix contains the correction factors for the external Higgs bosons $\{h_1, h_2, h_3\}$ relative to the lowest-order mass eigenstates $\{h, H, A\}$. The matrix elements \hat{Z}_{aj} [8, 15, 16] are composed of the root of the external wave function normalisation factor \hat{Z}_i^a and the on-shell transition ratio \hat{Z}_{ij}^a ,

$$\hat{Z}_i^a := \text{Res}_{\mathcal{M}_a^2} \{ \Delta_{ii}(p^2) \}, \quad \hat{Z}_{ij}^a = \frac{\Delta_{ij}(p^2)}{\Delta_{jj}(p^2)} \bigg|_{p^2=\mathcal{M}_a^2}, \quad (2)$$

which are evaluated at the complex pole \mathcal{M}_a^2 . Here, Δ_{ij} are the propagators, $\{a, b, c\}$ denote the loop-corrected mass eigenstates, and $\{i, j, k\}$ refer to the tree-level mass eigenstates. With an appropriate assignment of the indices of the two types of states (see Ref. [8]), the matrix elements can be written as

¹ The full mixing at higher orders takes place not just between $\{h, H, A\}$, but also with the Goldstone boson and the electroweak gauge bosons. Their impact is minimal for the processes considered here and, therefore, neglected in our treatment of the loop-corrected Higgs bosons, see Refs. [3, 4] for a discussion.

$$\hat{\mathbf{Z}}_{aj} = \sqrt{\hat{\mathbf{Z}}_a} \hat{\mathbf{Z}}_{aj}. \quad (3)$$

Using the $\hat{\mathbf{Z}}$ matrix elements, we obtain an expression for the amplitude of the loop-corrected mass eigenstates h_a as a linear combination of the amplitudes of the tree-level states as follows²:

$$\mathcal{A}_{h_a} = \hat{\mathbf{Z}} \begin{pmatrix} \mathcal{A}_h \\ \mathcal{A}_H \\ \mathcal{A}_A \end{pmatrix} = \hat{\mathbf{Z}}_{ah} \mathcal{A}_h + \hat{\mathbf{Z}}_{aH} \mathcal{A}_H + \hat{\mathbf{Z}}_{aA} \mathcal{A}_A + \dots \quad (4)$$

3. Higgs production cross sections in the MSSM with complex parameters

For low and medium values of $\tan \beta$ in the MSSM, Higgs bosons are predominantly produced through gluon fusion. At high $\tan \beta$, the production in association with a pair of bottom quarks is the dominant process, due to the enhanced bottom-Yukawa coupling to the Higgs bosons. In the following sections, we will present cross sections for production of Higgs bosons h_1, h_2 and h_3 in the MSSM via gluon fusion and bottom quark annihilation for a general case of arbitrary complex parameters.

In the MSSM, the most significant contributions to the gluon-fusion cross section arise from top, bottom, stop and sbottom loops. Moreover, the weights of the top- and bottom-loop contributions have to be modified by the relative couplings to the MSSM Higgs bosons. For the case of the MSSM with complex parameters, \mathcal{CP} -violating phases can enter the cross section calculation via the $\hat{\mathbf{Z}}$ factors, Higgs-squark couplings, and through $\tan \beta$ -resummed Δ_b corrections. These Δ_b corrections make the effective bottom Yukawa couplings explicitly complex, leading to $g_{b_L}^\phi \neq g_{b_R}^\phi$ (see Refs. [3, 4] for a discussion). Additionally, \mathcal{CP} -violating phases give rise to non-vanishing couplings of squarks to the \mathcal{CP} -odd state A , g_{fii}^A , which are zero when \mathcal{CP} is conserved.

The leading order (LO) production cross section of the mass eigenstates h_a can be written as follows:

$$\sigma_{\text{LO}}(pp \rightarrow h_a) = \sigma_0^{h_a} \tau_{h_a} \mathcal{L}^{gg}(\tau_{h_a}) \quad \text{with} \quad \mathcal{L}^{gg}(\tau) = \int_{\tau}^1 \frac{dx}{x} g(x) g(\tau/x), \quad (5)$$

where $\tau_{h_a} = M_{h_a}^2/s$. The hadronic squared centre-of-mass energy is denoted by s , and \mathcal{L}^{gg} denotes the gluon-gluon luminosity. The partonic LO cross

² The ellipsis denote mixing contributions from the Goldstone bosons and electroweak gauge bosons which have been neglected.

section for $gg \rightarrow h_a$ is given by

$$\sigma_0^{h_a} = \frac{G_F \alpha_s^2}{288 \sqrt{\pi}} \left[\left| \mathcal{A}^{h_a, e} \right|^2 + \left| \mathcal{A}^{h_a, o} \right|^2 \right]$$

with $\mathcal{A}^{h_a, e} = \hat{\mathbf{Z}}_{ah} \mathcal{A}_+^h + \hat{\mathbf{Z}}_{aH} \mathcal{A}_+^H + \hat{\mathbf{Z}}_{aA} \mathcal{A}_+^A$
 and $\mathcal{A}^{h_a, o} = \hat{\mathbf{Z}}_{ah} \mathcal{A}_-^h + \hat{\mathbf{Z}}_{aH} \mathcal{A}_-^H + \hat{\mathbf{Z}}_{aA} \mathcal{A}_-^A$, (6)

where G_F is Fermi's constant, and $\hat{\mathbf{Z}}_{a\phi}$ are the elements of the $\hat{\mathbf{Z}}$ matrix. The “LO cross section” is the cross section for the diagrams in Fig. 1 despite the fact that it contains higher-order effects through the application of the $\hat{\mathbf{Z}}$ factors. We see from Eq. (6) that the final polarisation and colour averaged squared loop amplitude for a mass eigenstate h_a consists of two non-interfering squared amplitudes. This is due to the different tensor structures of various contributions. The amplitudes contributing to $\mathcal{A}^{h_a, e}$ have a symmetric tensor structure, while those contributing to $\mathcal{A}^{h_a, o}$ have an anti-symmetric one. This results in the cross section being expressible as the sum of two non-interfering squared amplitudes. This also explains the naming of the first and the second term with $\mathcal{A}^{h_a, e}$, where “e” denotes “even”, and $\mathcal{A}^{h_a, o}$, where “o” denotes “odd”, respectively. Using this, we can split σ_{LO} into σ_{LO}^e and σ_{LO}^o .

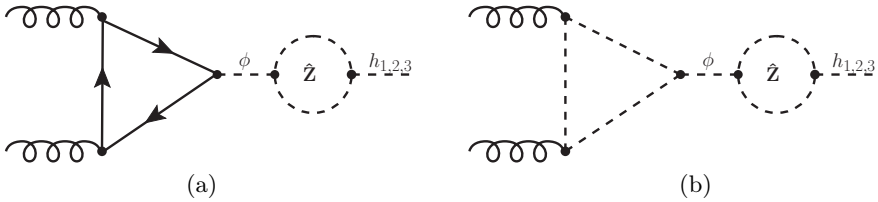


Fig. 1. Feynman diagrams for the LO cross section with (a) quark and (b) squark contributions.

For the two \mathcal{CP} -even tree-level mass eigenstates $\phi^e \in \{h, H\}$, the amplitudes are

$$\mathcal{A}_+^{\phi^e} = \sum_{q \in \{t, b\}} \left(a_{q,+}^{\phi^e} + \tilde{a}_q^{\phi^e} \right), \quad \mathcal{A}_-^{\phi^e} = \sum_{q \in \{t, b\}} a_{q,-}^{\phi^e}. \quad (7)$$

Similarly, for the \mathcal{CP} -odd Higgs boson A , the amplitudes are

$$\mathcal{A}_-^A = \sum_{q \in \{t, b\}} \left(a_{q,-}^A + \tilde{a}_q^A \right), \quad \mathcal{A}_+^A = \sum_{q \in \{t, b\}} a_{q,+}^A. \quad (8)$$

In the above expressions, $a_{q,+}^{\phi}$ and $a_{q,-}^{\phi}$ ($\phi \in \{h, H, A\}$) are the loop amplitudes for quark contributions proportional to the sum and difference of the

right- and left-handed Yukawa couplings, respectively. The terms \tilde{a}_q^ϕ denote the loop amplitudes of squark contributions. The full expressions for $a_{q,\pm}^\phi$ and \tilde{a}_q^ϕ can be found in Ref. [3].

The leading order cross section can be supplemented by higher-order corrections. At next-to-leading order (NLO), the hadronic cross section is given by the expression

$$\begin{aligned} \sigma_{\text{NLO}}^{e/o}(pp \rightarrow h_a + X) = & \sigma_0^{h_a, e/o} \tau_{h_a} \mathcal{L}^{gg}(\tau_{h_a}) \left[1 + C^{e/o} \frac{\alpha_s}{\pi} \right] \\ & + \Delta\sigma_{gg}^{e/o} + \Delta\sigma_{gq}^{e/o} + \Delta\sigma_{q\bar{q}}^{e/o}. \end{aligned} \quad (9)$$

The $\Delta\sigma$ terms contain the real corrections from the production of a Higgs boson in association with a gluon or quark jet. Note that the different left- and right-handed Yukawa couplings arise only for the case of the bottom quark due to the incorporation of the full Δ_b resummation, which makes the couplings explicitly complex at leading order [16, 17]. Beyond the leading order, we use a simplified Δ_b resummation which makes the left- and right-handed bottom Yukawa couplings equivalent to each other. Due to this, in the amplitudes for real corrections in the case of the MSSM with complex parameters, the only new ingredients, aside from the \hat{Z} factors, are Higgs-squark couplings $g_{\tilde{q}ii}^A$, which are added to the \mathcal{CP} -even components $\Delta\sigma^e$. The real corrections can be split in $\Delta\sigma^e$ and $\Delta\sigma^o$ since no interference terms arise.

In the MSSM with real parameters, analytical NLO virtual contributions involving squarks, quarks and gluinos are either known in the limit of a vanishing Higgs mass [18–21] or in an expansion of heavy SUSY masses [22–24]. In the MSSM with complex parameters, the virtual contributions containing quarks have a similar structure as for those in the MSSM with real parameters, owing to the simplified Δ_b approximation beyond LO. However, contributions from virtual corrections involving squarks are more difficult to generalise to complex parameters. We, therefore, interpolate these NLO virtual contributions between phases 0 and π of the various MSSM parameters using a cosine interpolation [25, 26]. For a certain value of the phase ϕ_z of a complex parameter z , the virtual NLO amplitude $\mathcal{A}_{\text{NLO}}^\phi(\phi_z)$ can be approximated using

$$\mathcal{A}_{\text{NLO}}^\phi(\phi_z) = \frac{1 + \cos \phi_z}{2} \mathcal{A}_{\text{NLO}}^\phi(0) + \frac{1 - \cos \phi_z}{2} \mathcal{A}_{\text{NLO}}^\phi(\pi) \quad (10)$$

for each of the lowest-order mass eigenstates $\phi \in \{h, H, A\}$. Here, $\mathcal{A}_{\text{NLO}}^\phi(0)$ is the analytical result for the MSSM with real parameters, and $\mathcal{A}_{\text{NLO}}^\phi(\pi)$ is the analytical result with $z \rightarrow -z$. Finally, we also account for two-loop electroweak (EW) corrections mediated by light quarks, which are re-weighted to the MSSM with complex parameters. The total gluon-fusion

cross section at the k^{th} order is the sum of the two parts

$$\sigma_{\text{N}^k\text{LO}}(pp \rightarrow h_a + X) = \sigma_{\text{N}^k\text{LO}}^e(pp \rightarrow h_a + X) + \sigma_{\text{N}^k\text{LO}}^o(pp \rightarrow h_a + X), \quad (11)$$

and the result beyond LO QCD is obtained through

$$\sigma_{\text{N}^k\text{LO}}^e = \sigma_{\text{NLO}}^e \left(1 + \delta_{\text{EW}}^{\text{lf}} \right) + \left(\sigma_{\text{N}^k\text{LO},\text{EFT}}^{t,e} - \sigma_{\text{NLO},\text{EFT}}^{t,e} \right), \quad (12)$$

$$\sigma_{\text{N}^k\text{LO}}^o = \sigma_{\text{NLO}}^o + \left(\sigma_{\text{N}^k\text{LO},\text{EFT}}^{t,o} - \sigma_{\text{NLO},\text{EFT}}^{t,o} \right), \quad (13)$$

with $\delta_{\text{EW}}^{\text{lf}}$ containing the EW corrections from light fermions. N^3LO QCD corrections are only taken into account for the \mathcal{CP} -even component of the light Higgs boson, allowing us to match the precision of the light Higgs boson cross section in the SM used in up-to-date predictions. This is because the light Higgs boson that is identified with the observed signal at 125 GeV is usually assumed to have a dominant \mathcal{CP} -even component, which is also the case in the scenarios which we consider in our numerical discussion. For the \mathcal{CP} -odd component of the light Higgs and the heavy Higgs bosons, we employ NNLO corrections for the top-quark induced contributions in the effective theory of a heavy top-quark. This means that we do not account for top-quark mass effects beyond NLO, but only factor out the LO QCD cross sections $\sigma_{\text{LO}}^{t,e}$ and $\sigma_{\text{LO}}^{t,o}$. These results have been implemented in an extension of the FORTRAN code **SusHi** [27, 28], called **SusHiMi** (SUsymmetric Higgs MIXing) and are currently the state-of-the-art for neutral Higgs production in the MSSM with complex parameters [3]. **SusHiMi** will be included in the next release of **SusHi**.

Finally, for the production of the Higgs boson h_a via bottom-quark annihilation in the MSSM with complex parameters, as implemented in **SusHiMi**, the results for the SM Higgs boson are re-weighted to the MSSM with $|\hat{\mathbf{Z}}_{ah}g_b^h + \hat{\mathbf{Z}}_{aH}g_b^H|^2 + |\hat{\mathbf{Z}}_{aA}g_b^A|^2$, which includes $\tan\beta$ -enhanced squark effects through Δ_b using the simplified Δ_b resummation.

We carry out our numerical analysis in a slightly modified version of the classic MSSM scenario introduced in Ref. [29], named the $m_h^{\text{mod}+}$ scenario. For this $m_h^{\text{mod}+}$ -inspired scenario, we choose for vanishing phases of the complex parameters:

$$\begin{aligned} M_1 &= 250 \text{ GeV}, & M_2 &= 500 \text{ GeV}, & M_3 &= 1.5 \text{ TeV} \\ X_t &= X_b = X_\tau = 1.5 \text{ TeV}, & A_q &= A_l = 0 \\ \mu &= \tilde{m}_Q = \tilde{m}_L = 1 \text{ TeV}. \end{aligned} \quad (14)$$

For the SM parameters, we use the values $m_t^{\text{OS}} = 173.20 \text{ GeV}$, $m_b^{\overline{\text{MS}}}(m_b) = 4.16 \text{ GeV}$, $m_b^{\text{OS}} = 4.75 \text{ GeV}$ and $\alpha_s(M_Z) = 0.119$. Furthermore, we choose

$\tan\beta = 10$ and $M_{H^\pm} = 900$ GeV. The $m_h^{\text{mod}+}$ -inspired scenario features a lightest Higgs h_1 which is mostly \mathcal{CP} -even and SM-like with a mass close to 125 GeV, and two heavier Higgs bosons h_2 and h_3 which are nearly mass-degenerate and heavily admixed. In our numerical analyses, we employ **FeynHiggs-2.11.2** [30–34] to calculate Higgs masses and $\hat{\mathbf{Z}}$ factors. In the following, we study the variation of Higgs masses and cross sections with the phase of A_t . The phase ϕ_{A_t} is varied from 0 to 2π leaving the absolute value $|A_t|$ constant in order to address various aspects in the phenomenology of Higgs boson production³.

The variation of masses and \mathcal{CP} -character of the Higgs states h_2 and h_3 with ϕ_{A_t} is depicted in Fig. 2 (a). We call the mass eigenstates h_2 and h_3 either h_e or h_o , depending on their mixing character: if $|\hat{\mathbf{Z}}_{aA}|^2 \gtrsim 1/2$, the mass eigenstate h_a is denoted by h_o , otherwise it is denoted by h_e . We see from the lower panel of Fig. 2 (a) that while h_3 (grey/green) is

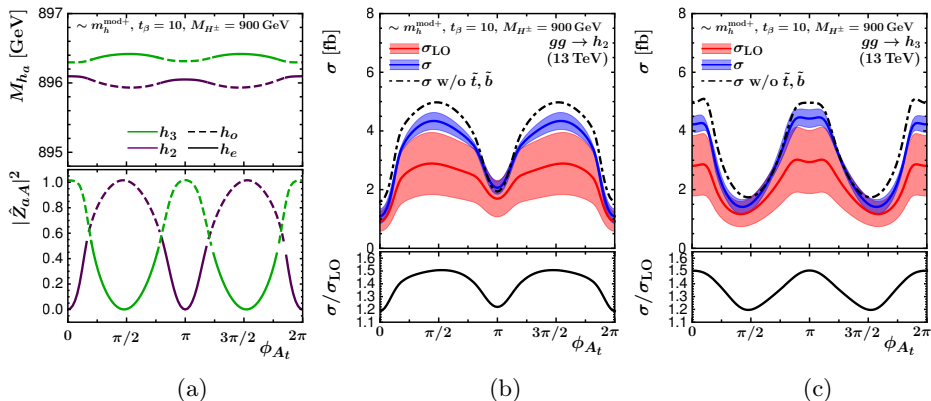


Fig. 2. (Colour on-line) Masses, mixing and gluon-fusion cross sections of h_2 and h_3 in the $m_h^{\text{mod}+}$ -inspired scenario with $\tan\beta = 10$. (a) Upper panel: Variation of h_2 (black/violet, lower curve) and h_3 (grey/green, upper curve) masses in GeV with ϕ_{A_t} . Lower panel: The \mathcal{CP} -odd character $|\hat{\mathbf{Z}}_{aA}|^2$ as a function of ϕ_{A_t} . The solid and dashed curves represent regions in ϕ_{A_t} where h_2 and h_3 are predominantly \mathcal{CP} -even (h_e) or -odd (h_o), respectively. At $\phi_{A_t} = 0$, the state h_3 (grey/green) is fully \mathcal{CP} -odd whereas h_2 (black/violet) is fully \mathcal{CP} -even. (b), (c) LO (lowest red curve) and best prediction (middle blue curve) for the gluon-fusion cross section for (b) h_2 and (c) h_3 in fb as a function of ϕ_{A_t} . The black dot-dashed curve depicts the best prediction for the cross section without squark contributions (except through $\hat{\mathbf{Z}}$ factors). In the lower panel, we show the K -factor $\sigma/\sigma_{\text{LO}}$.

³ We display the full range of the phase without imposing EDM constraints, following the common approach in studies of Higgs phenomenology with \mathcal{CP} -violation. See Refs. [35, 36] for a recent discussion.

fully \mathcal{CP} -odd ($|\hat{\mathbf{Z}}_{aA}|^2 \sim 1$)⁴ at $\phi_{A_t} = 0$, and h_2 (black/violet) is fully \mathcal{CP} -even ($|\hat{\mathbf{Z}}_{aA}|^2 \sim 0$) at $\phi_{A_t} = 0$, their \mathcal{CP} -character varies widely as we scan through ϕ_{A_t} , with both of them being substantially admixed for large parts of the ϕ_{A_t} -space. Figure 2 (b) and (c) depicts the cross sections for gluon fusion production of h_2 and h_3 in fb. The lowest (red) curves with the larger renormalisation and factorisation scale uncertainties associated with them show the variation of the LO cross section with ϕ_{A_t} . The middle (blue) curves with the reduced scale uncertainties show our best prediction cross section, whereas the black dot-dashed curves depict the cross section with the squark contributions from loops turned off. Therefore, the only squark contributions to the black dot-dashed curve come from the $\hat{\mathbf{Z}}$ factors. One notices that the middle (blue) (best prediction) curve and the dot-dashed curves follow each other closely and have a similar magnitude of the cross section. This implies that in this scenario, the phase dependence of the cross section comes mostly from the $\hat{\mathbf{Z}}$ factors, and not directly from squark loops. Moreover, the phase dependence of the cross sections closely follows the \mathcal{CP} -character of the Higgs states in Fig. 2 (a). The lower panels of the cross section curves show the K -factors, which lie between about 1.2 and 1.5 with the phase ϕ_{A_t} and follow the variation the mixing character of h_3 and h_3 .

Note that the curves for the cross sections of h_2 and h_3 have complementary shapes, and the two Higgs bosons are nearly mass degenerate. In such a case of nearly mass degenerate Higgs bosons, it may not be possible to experimentally resolve the two states as separate signals. The experimentally measured quantity would be the sum of the cross sections times their branching ratios along with the interference contributions in the full process of Higgs production and decay. We will explore the effects of these \mathcal{CP} -violating interference contributions in the next section.

4. Impact of interference contributions

At the LHC, so far all searches for additional heavy Higgs bosons that have been interpreted in specific scenarios assume that the signal contributions from different Higgs bosons can be added incoherently, *i.e.* without any interference effects, which is a valid assumption for the case of \mathcal{CP} -conservation because the h - H interference becomes large only in a small and already deeply excluded region of parameter space. However, if we allow for \mathcal{CP} violation, all three loop-corrected mass eigenstates $h_a, a \in \{1, 2, 3\}$ can interfere. Such interference effects are especially significant when the mass splitting between the Higgs bosons is smaller than the sum of their to-

⁴ Note that since the $\hat{\mathbf{Z}}$ matrix is non-unitary, its elements can have a value greater than 1.

tal widths, in which case the resonances can overlap. In order to accurately interpret the experimental limits on $\sigma \times \text{BR}$ from Higgs searches at the LHC, it is, therefore, crucial to also account for these interference contributions in their predictions, which could significantly enhance or diminish the value of $\sigma \times \text{BR}$ in comparison to their values for the \mathcal{CP} -conserving case.

We now consider a full process of Higgs production and decay, and calculate the interference of amplitudes in an s -channel exchange of the Higgses h_1, h_2 and h_3 in a generic $2 \rightarrow 2$ parton level process $I \rightarrow h_1, h_2, h_3 \rightarrow F$, with the initial state I denoting the production process and final state F denoting the decay products. Later on, we will apply this to specific production and decay mechanisms. The calculation of the interference factors is carried out at leading order taking into account Higgs masses, total widths, and \hat{Z} factors from **FeynHiggs-2.13.0** computed with full one-loop and leading two-loop contributions. State-of-the-art higher-order contributions are taken into account in the computation for production cross sections for I and branching ratios for F . For the QCD corrections, a factorisation of higher-order corrections between initial and final states is often justified. This only misses corrections connecting initial- and final-state particles. Therefore it is well-motivated to apply the interference factor calculated at LO only, with the full process containing higher-order corrections.

The interference term for a process $I \rightarrow F$ with $h_{1,2,3}$ Higgs exchange is obtained from the difference between the coherent and incoherent sum of the $2 \rightarrow 2$ squared amplitudes [6–8]

$$|\mathcal{A}|_{\text{int}}^2 = |\mathcal{A}|_{\text{coh}}^2 - |\mathcal{A}|_{\text{incoh}}^2, \quad (15)$$

where the coherent and incoherent sums are defined as

$$|\mathcal{A}|_{\text{coh}}^2 = \left| \sum_{a=1}^3 \mathcal{A}_{h_a} \right|^2, \quad |\mathcal{A}|_{\text{incoh}}^2 = \sum_{a=1}^3 |\mathcal{A}_{h_a}|^2. \quad (16)$$

The squared amplitudes in Eq. (15) and Eq. (16) can be used to define the cross sections $\sigma_{\text{int}}, \sigma_{\text{coh}}$ and σ_{incoh} . The relative interference term for the cross section of the full process is then defined as

$$\eta^{IF} = \frac{\sigma_{\text{int}}^{IF}}{\sigma_{\text{incoh}}^{IF}}. \quad (17)$$

The total interference contribution to the process can be expressed as $\sigma_{\text{int}} = \sigma_{\text{int}_{12}} + \sigma_{\text{int}_{23}} + \sigma_{\text{int}_{13}}$, where $\sigma_{\text{int}_{ab}}$ denotes the interference term between h_a and h_b . We then define the relative contribution for a *single* Higgs h_a from its interference with the Higgses h_b and h_c as

$$\eta_a^{IF} = \frac{\sigma_{\text{int}_{ab}}^{IF}}{\sigma_{h_a}^{IF} + \sigma_{h_b}^{IF}} + \frac{\sigma_{\text{int}_{ac}}^{IF}}{\sigma_{h_a}^{IF} + \sigma_{h_c}^{IF}}. \quad (18)$$

Using η_a^{IF} , we can approximately factorise the experimentally measurable (coherent) cross section as [6–8]

$$\sigma(pp \rightarrow I \rightarrow h_{1,2,3} \rightarrow F) \simeq \sum_{a=1}^3 \sigma(pp \rightarrow I \rightarrow h_a) (1 + \eta_a^{IF}) \text{BR}(h_a \rightarrow F). \quad (19)$$

Currently, **SuSHiMi** implements the relative interference factors for the heavy Higgs bosons, η_2^{IF} and η_3^{IF} , for the case where only h_2 and h_3 interfere using Eq. (18) [4].

In the following, we will study the effects of interference between h_2 and h_3 in the $b\bar{b} \rightarrow \tau^+\tau^-$ process. For this purpose, we define a benchmark scenario, which we name $\mathcal{CP}\text{Int}$. Similar to the $m_h^{\text{mod}+}$ -inspired scenario, the $\mathcal{CP}\text{Int}$ scenario contains an SM-like lightest Higgs, and two nearly mass degenerate and strongly admixed heavy Higgs bosons h_2 and h_3 . Since h_1 is mostly \mathcal{CP} -even and has a large mass splitting from $h_{2,3}$, we only consider the interference between the two heavy Higgs bosons. The $\mathcal{CP}\text{Int}$ scenario is defined with the following parameter values:

$$\begin{aligned} M_{\text{SUSY}} &= 1.5 \text{ TeV}, & \mu &= 1.5 \text{ TeV}, \\ M_1 &= 0.5 \text{ TeV}, & M_2 &= 1 \text{ TeV}, & M_3 &= 2.5 e^{i\frac{\pi}{3}} \text{ TeV}, \\ A_t &= \left(\frac{\mu}{\tan\beta} + 1.8 M_{\text{SUSY}} \right) e^{i\frac{\pi}{4}}, & A_b &= A_t, & A_\tau &= |A_t|, \\ M_{U_3} &= M_{Q_3} = M_{D_3} = M_{\text{SUSY}}, & M_{L_{1,2}} &= M_{E_{1,2}} = 0.5 \text{ TeV}. \end{aligned} \quad (20)$$

The SM input parameters are $M_W = 80.385 \text{ GeV}$, $M_Z = 91.1876 \text{ GeV}$, $m_t^{\text{OS}} = 172.5 \text{ GeV}$, $m_b^{\text{MS}}(m_b) = 4.18 \text{ GeV}$, and $\alpha_s(m_Z) = 0.118$, in accordance with the recommendations in Ref. [37]. The phases of the parameters $A_t = A_b$ and M_3 have been chosen to be non-maximal in view of the impact of bounds from EDMs. This benchmark illustrates the effects of mixing and interference in h_2, h_3 production and decay. A more detailed study of the EDM constraints will follow in a forthcoming publication [36].

In Fig. 3 (a), we show the relative interference factors $\eta^{b\bar{b},\tau\tau}$ for $b\bar{b} \rightarrow h_2, h_3 \rightarrow \tau^+\tau^-$ in the $(M_{H^\pm}, \tan\beta)$ plane. As a result of the mass degeneracy between h_2 and h_3 and the fact that they are highly \mathcal{CP} -admixed, the interference contribution in their coherent $\sigma \times \text{BR}$ is strongly destructive, with $\eta^{b\bar{b},\tau\tau}$ reaching a minimum of almost -98% in parts of the parameter space. This can be seen in Fig. 3 (a), where we observe a valley of strong destructive interference of about -90% starting from around the points $(550 \text{ GeV}, 20)$ to $(1000 \text{ GeV}, 11)$ in the parameter plane. Figure 3 (b) depicts the theoretical predictions for $\sigma(pp \rightarrow b\bar{b} \rightarrow h_2, h_3 \rightarrow \tau^+\tau^-)$ as a function of the mass M_{h_a} of a neutral scalar resonance h_a , along with the respective experimental limits for the production of a single resonance ϕ at mass M_ϕ obtained

from ATLAS searches for neutral Higgs bosons in Run 2 at 13 TeV with $\int \mathcal{L} = 13.3 \text{ fb}^{-1}$ reported in Ref. [38]. The black curves represent essentially model-independent upper limits on the $b\bar{b}$ production cross section times the $\tau^+\tau^-$ branching ratio of a scalar boson *versus* its mass. The solid black line represents the observed exclusion bound and the dotted black line depicts the expected bound. The theoretical predictions have been plotted for a sample of $\tan\beta$ values as a function of $M_{h_a} = M_{h_3}$, where in the relevant regions we also have $M_{h_3} \simeq M_{h_2}$. The top-most curve (red) for the predicted $\sigma \times \text{BR}$ corresponds to $\tan\beta = 18$, while the bottom-most one (violet) corresponds to $\tan\beta = 13$. The comparison of the interference-corrected $\sigma \times \text{BR}$ with the experimental limits can be understood as follows: the M_{h_a} values corresponding to the parts of the predicted curves that lie *above* the black experimentally measured curves are excluded at 95% C.L., while those corresponding to the parts that lie below the experimental curves are still allowed. With this understanding, we can infer that for certain values of $\tan\beta$, the destructive interference suppresses the predicted $\sigma \times \text{BR}$ below the experimental limits such that values of Higgs masses that would have been excluded if the interference contributions had not been taken into account are now allowed.

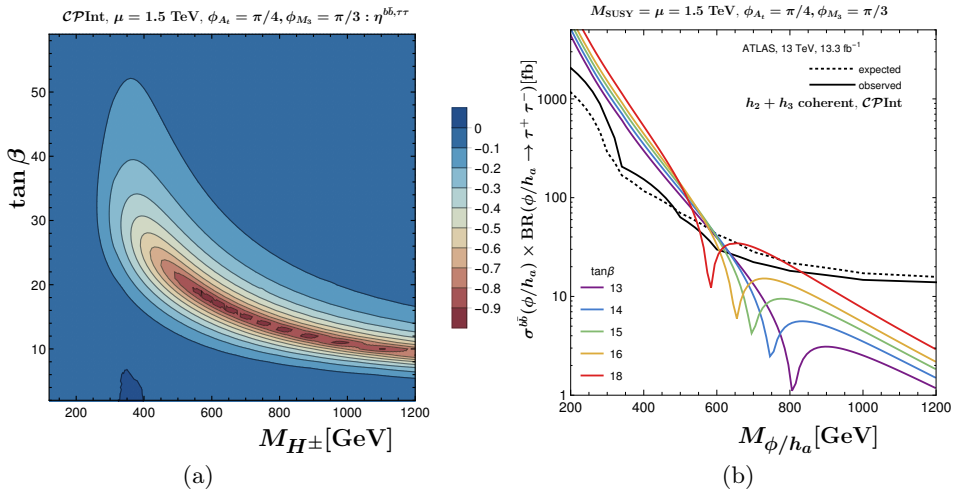


Fig. 3. (Colour on-line) Interference effects in the $b\bar{b} \rightarrow h_2, h_3 \rightarrow \tau^+\tau^-$ channel: (a) Contour plot for the interference factor $\eta^{b\bar{b},\tau\tau}$ in the $(M_{H^\pm}, \tan\beta)$ plane, and (b) comparison of $\sigma \times \text{BR}$ (in fb) for h_2 and h_3 including interference effects in the \mathcal{CPInt} scenario with the 95 % C.L. exclusion bounds obtained by ATLAS at 13 TeV [38].

Finally, we analyse the exclusion limits in the $(M_{H^\pm}, \tan\beta)$ plane using the program **HiggsBounds-5.1.1beta** [39–42]. For any particular model, **HiggsBounds** takes a selection of Higgs sector predictions as input and uses the experimental topological cross-section limits from Higgs searches at LEP, the Tevatron and the LHC to determine whether this parameter point has been excluded at 95% C.L. In order to incorporate the interference effects into the prediction of $\sigma(b\bar{b} \rightarrow h_a)$ times the respective branching ratio, the ratio $\frac{\sigma^{\text{model}}}{\sigma_{\text{SM}}}$ of production cross sections which are used as input to **HiggsBounds** are rescaled with the interference factor⁵. In Fig. 4, we show the modified exclusion bounds in the $(M_{H^\pm}, \tan\beta)$ plane, overlayed with m_{h_1} contours. We see that accounting for the interference term and the complex parameters in the $\sigma \times \text{BR}$ prediction leads to a “fjord” of destructive interference in the region between $M_{H^\pm} \sim 550$ GeV and 800 GeV for $\tan\beta \sim 13$ to 20 that remains unexcluded due to the suppression of the predicted $\sigma \times \text{BR}$. It is worthwhile to note that $M_{h_1} \sim 125$ GeV in this unexcluded space, making it a phenomenologically important region.

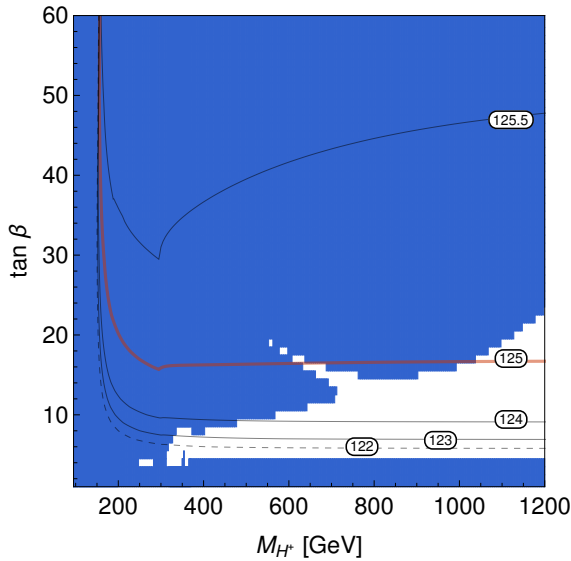


Fig. 4. Exclusion bounds in the $(M_{H^\pm}, \tan\beta)$ plane obtained with **HiggsBounds5.1.1beta** for the \mathcal{CP} Int scenario. The grey/blue region depicts the exclusion bounds when interference terms in the production and decay of h_2 and h_3 are taken into account for $b\bar{b} \rightarrow \tau^+\tau^-$. The contour lines depict the mass M_{h_1} (in GeV) of the lightest Higgs boson.

⁵ In the new version of **HiggsBounds**, the interference factors can be directly given as an input.

5. Conclusions

Complex parameters in the MSSM give rise to rich and interesting phenomenology in the Higgs sector. Not only are such complex parameters needed for explaining the matter–antimatter asymmetry of the universe, they can also be extremely relevant for Higgs searches at the LHC. We presented the full LO cross section for gluon fusion supplemented with various higher-order contributions, and examined the three ways in which complex parameters affect the cross section, namely via $\hat{\mathbf{Z}}$ factors, complex Yukawa couplings due to Δ_b corrections, and Higgs–squark couplings. The bottom–quark annihilation cross section was treated with a simple re-weighting procedure. Using the $m_h^{\text{mod}+}$ -inspired scenario, we demonstrated the effects of \mathcal{CP} -violating Higgs mixing on the gluon-fusion Higgs production cross sections, and motivated the need to include interference contributions in the predictions for the $\sigma \times \text{BR}$ of a full process of Higgs production and decay. Furthermore, we reviewed a formalism to consistently include such interference effects in our theoretical predictions and showed that taking into account \mathcal{CP} -violating mixing and interference contributions can significantly alter exclusion bounds from the LHC. It is, therefore, essential to allow for the possibility that the MSSM Higgs sector may not be \mathcal{CP} -conserving when interpreting the latest data from LHC Run 2.

The authors acknowledge support by Deutsche Forschungsgemeinschaft through the SFB 676 “Particles, Strings and the Early Universe” and by the European Commission through the “HiggsTools” Initial Training Network PITN-GA-2012-316704.

REFERENCES

- [1] G. Aad *et al.* [ATLAS Collaboration], *Phys. Lett. B* **716**, 1 (2012) [arXiv:1207.7214 [hep-ex]].
- [2] S. Chatrchyan *et al.* [CMS Collaboration], *Phys. Lett. B* **716**, 30 (2012) [arXiv:1207.7235 [hep-ex]].
- [3] S. Liebler, S. Patel, G. Weiglein, *Eur. Phys. J. C* **77**, 305 (2017) [arXiv:1611.09308 [hep-ph]].
- [4] S. Patel, Ph.D. Thesis, University of Hamburg, Hamburg, 2017, DOI: 10.3204/PUBDB-2017-11438.
- [5] A. Fowler, Ph.D. Thesis, Durham, IPPP, 2010.
- [6] E. Fuchs, Ph.D. Thesis, University of Hamburg, Dept. Phys., Hamburg, 2015, DOI: 10.3204/DESY-THESIS-2015-037.

- [7] E. Fuchs, G. Weiglein, *Eur. Phys. J. C* **78**, 87 (2018) [arXiv:1705.05757 [hep-ph]].
- [8] E. Fuchs, G. Weiglein, *J. High Energy Phys.* **1709**, 079 (2017) [arXiv:1610.06193 [hep-ph]].
- [9] D.A. Demir *et al.*, *Nucl. Phys. B* **680**, 339 (2004) [arXiv:hep-ph/0311314].
- [10] D. Chang, W.-Y. Keung, A. Pilaftsis, *Phys. Rev. Lett.* **82**, 900 (1999) [arXiv:hep-ph/9811202].
- [11] A. Pilaftsis, *Phys. Lett. B* **471**, 174 (1999) [arXiv:hep-ph/9909485].
- [12] P.H. Chankowski, S. Pokorski, J. Rosiek, *Nucl. Phys. B* **423**, 437 (1994) [arXiv:hep-ph/9303309].
- [13] A. Dabelstein, *Nucl. Phys. B* **456**, 25 (1995) [arXiv:hep-ph/9503443].
- [14] S. Heinemeyer, W. Hollik, J. Rosiek, G. Weiglein, *Eur. Phys. J. C* **19**, 535 (2001) [arXiv:hep-ph/0102081].
- [15] K.E. Williams, G. Weiglein, *Phys. Lett. B* **660**, 217 (2008) [arXiv:0710.5320 [hep-ph]].
- [16] K.E. Williams, H. Rzehak, G. Weiglein, *Eur. Phys. J. C* **71**, 1669 (2011) [arXiv:1103.1335 [hep-ph]].
- [17] J. Baglio *et al.*, *Comput. Phys. Commun.* **185**, 3372 (2014) [arXiv:1312.4788 [hep-ph]].
- [18] R.V. Harlander, M. Steinhauser, *Phys. Lett. B* **574**, 258 (2003) [arXiv:hep-ph/0307346].
- [19] R.V. Harlander, M. Steinhauser, *J. High Energy Phys.* **0409**, 066 (2004) [arXiv:hep-ph/0409010].
- [20] R.V. Harlander, F. Hofmann, *J. High Energy Phys.* **0603**, 050 (2006) [arXiv:hep-ph/0507041].
- [21] G. Degrassi, P. Slavich, *Nucl. Phys. B* **805**, 267 (2008) [arXiv:0806.1495 [hep-ph]].
- [22] G. Degrassi, P. Slavich, *J. High Energy Phys.* **1011**, 044 (2010) [arXiv:1007.3465 [hep-ph]].
- [23] G. Degrassi, S. Di Vita, P. Slavich, *J. High Energy Phys.* **1108**, 128 (2011) [arXiv:1107.0914 [hep-ph]].
- [24] G. Degrassi, S. Di Vita, P. Slavich, *Eur. Phys. J. C* **72**, 2032 (2012) [arXiv:1204.1016 [hep-ph]].
- [25] S. Heinemeyer *et al.*, *J. High Energy Phys.* **0608**, 052 (2006) [arXiv:hep-ph/0604147].
- [26] T. Hahn *et al.*, in: SUSY 2007 Proceedings, 15th International Conference on Supersymmetry and Unification of Fundamental Interactions, Karlsruhe, Germany, July 26–August 1, 2007, pp. 442–449 [arXiv:0710.4891 [hep-ph]].
- [27] R.V. Harlander, S. Liebler, H. Mantler, *Comput. Phys. Commun.* **184**, 1605 (2013) [arXiv:1212.3249 [hep-ph]].
- [28] R.V. Harlander, S. Liebler, H. Mantler, *Comput. Phys. Commun.* **212**, 239 (2017) [arXiv:1605.03190 [hep-ph]].

- [29] M. Carena *et al.*, *Eur. Phys. J. C* **73**, 2552 (2013) [arXiv:1302.7033 [hep-ph]].
- [30] S. Heinemeyer, W. Hollik, G. Weiglein, *Comput. Phys. Commun.* **124**, 76 (2000) [arXiv:hep-ph/9812320].
- [31] S. Heinemeyer, W. Hollik, G. Weiglein, *Eur. Phys. J. C* **9**, 343 (1999) [arXiv:hep-ph/9812472].
- [32] G. Degrossi *et al.*, *Eur. Phys. J. C* **28**, 133 (2003) [arXiv:hep-ph/0212020].
- [33] M. Frank *et al.*, *J. High Energy Phys.* **0702**, 047 (2007) [arXiv:hep-ph/0611326].
- [34] T. Hahn *et al.*, *Phys. Rev. Lett.* **112**, 141801 (2014) [arXiv:1312.4937 [hep-ph]].
- [35] M. Carena *et al.*, *J. High Energy Phys.* **1602**, 123 (2016) [arXiv:1512.00437 [hep-ph]].
- [36] E. Fuchs *et al.*, in preparation.
- [37] D. de Florian *et al.* [LHC Higgs Cross Section Working Group], arXiv:1610.07922 [hep-ph].
- [38] ATLAS Collaboration, ATLAS-CONF-2016-085, CERN, Geneva, August 2016.
- [39] P. Bechtle *et al.*, *Eur. Phys. J. C* **75**, 421 (2015) [arXiv:1507.06706 [hep-ph]].
- [40] P. Bechtle *et al.*, *Eur. Phys. J. C* **74**, 2693 (2014) [arXiv:1311.0055 [hep-ph]].
- [41] P. Bechtle *et al.*, *Comput. Phys. Commun.* **181**, 138 (2010) [arXiv:0811.4169 [hep-ph]].
- [42] P. Bechtle *et al.*, *PoS CHARGED2012*, 024 (2012) [arXiv:1301.2345 [hep-ph]].